SENSOR ARRAY PROCESSING USING A UNITARY ROOT-MUSIC DIRECTION FINDING ALGORITHM

INVITED PAPER

Marius Pesavento *Alex B. Gershman* *Martin Haardt*

Department of ECE, McMaster University
Hamilton, Ontario, L8S 4K1 Canada
gershman@ieee.org

Siemens AG, ICN CA CTO 7
Hofmannstr. 51, Munich, Germany
Martin.Haardt@icn.siemens.de

ABSTRACT

We consider a computationally efficient unitary formulation of the popular root-MUSIC direction finding method. This technique is shown to reduce the computational demand of root-MUSIC, because it exploits the eigendecomposition of a real-valued covariance matrix. Closed-form expressions for the performance of the unitary root-MUSIC are derived. Additionally, results of computer simulations and real data processing are presented involving several benchmark array data sets. Our theoretical, numerical and experimental results show that unitary root-MUSIC has improved threshold and asymptotic performances relative to conventional root-MUSIC. As both the unitary and conventional root-MUSIC algorithms are applicable to the same array configuration – a uniform linear array, it can be recommended that unitary root-MUSIC should be always preferred by the user to conventional root-MUSIC.

1. INTRODUCTION

Recently, the problem of reducing the computational complexity of eigenstructure direction finding techniques via real-valued formulations has been addressed in the literature [1]-[3].

Below, a real-valued (unitary) formulation of the popular root-MUSIC direction finding algorithm [4] is presented. First, we show the exact equivalence of this technique to the so-called Forward-Backward (FB) root-MUSIC algorithm. We demonstrate, however, that unitary root-MUSIC has a simpler implementation than FB root-MUSIC because the former exploits the eigendecomposition of a real-valued matrix. Then, the asymptotic performance of unitary root-MUSIC is studied. We show that in situations with uncorrelated signal sources, the asymptotic performances of the unitary and conventional root-MUSIC algorithms are identical. However, in coherent source scenarios (occurring due to the multipath propagation effects), the asymptotic performance of unitary root-MUSIC is shown to be much better than that of conventional root-MUSIC. Simulation and experimental results are presented, which demonstrate that unitary root-MUSIC has better Signal to Noise Ratio (SNR) threshold than the conventional root-MUSIC algorithm. As both the unitary and conventional methods are applicable to the same array configuration – Uniform Linear Arrays (ULA's), it can be recommended that *unitary root-MUSIC should be always preferred by the user to conventional root-MUSIC.*

Supported by the Natural Sciences and Engineering Research Council (NSERC) of Canada.

2. ARRAY SIGNAL MODEL AND UNITARY ROOT-MUSIC

Assume that a ULA of M sensors receives q ($q < M$) narrowband signals impinging from the Directions of Arrival (DOA's) $\theta_1, \ldots, \theta_q$. Assume that there are N data snapshots $\mathbf{x}(1), \mathbf{x}(2), \ldots, \mathbf{x}(N)$ available. The $M \times 1$ array observation vector can be modeled as [4]

$$\mathbf{x}(t) = \mathbf{A}\mathbf{s}(t) + \mathbf{n}(t)\,, \tag{1}$$

where

$$\mathbf{A} = [\mathbf{a}(\theta_1), \ldots, \mathbf{a}(\theta_q)] \tag{2}$$

is the $M \times q$ direction matrix,

$$\mathbf{a}(\theta) = \left[1, e^{j\,(2\pi/\lambda)\,d\sin\theta}, \ldots, e^{j\,(2\pi/\lambda)\,d(M-1)\sin\theta}\right]^T \tag{3}$$

is the $M \times 1$ steering vector, $\mathbf{s}(t)$ is the $q \times 1$ vector of source waveforms, $\mathbf{n}(t)$ is the $M \times 1$ vector of white sensor noise, λ is the wavelength, d is the interelement spacing, and $(\cdot)^T$ stands for the transpose.

Define the $M \times M$ true and sample real-valued covariance matrices as [1]-[3]

$$\mathbf{C} = \mathbf{Q}^H \mathbf{R}_{\rm FB}\, \mathbf{Q}\,, \quad \hat{\mathbf{C}} = \mathbf{Q}^H \hat{\mathbf{R}}_{\rm FB}\, \mathbf{Q}\,, \tag{4}$$

where

$$\mathbf{R}_{\rm FB} = \frac{1}{2}(\mathbf{R} + \mathbf{J}\mathbf{R}^*\mathbf{J})\,, \quad \hat{\mathbf{R}}_{\rm FB} = \frac{1}{2}(\hat{\mathbf{R}} + \mathbf{J}\hat{\mathbf{R}}^*\mathbf{J}) \tag{5}$$

are the centro-Hermitian FB covariance matrix and its sample estimate, respectively. Here,

$$\mathbf{R} = \mathrm{E}\left\{\mathbf{x}(t)\mathbf{x}^H(t)\right\} = \mathbf{A}\mathbf{S}\mathbf{A}^H + \sigma^2\mathbf{I} \tag{6}$$

is the conventional complex-valued covariance matrix,

$$\hat{\mathbf{R}} = \frac{1}{N}\sum_{k=1}^{N} \mathbf{x}(k)\mathbf{x}^H(k) \tag{7}$$

is its sample estimate, $\mathbf{J}$ is the exchange matrix with ones on its antidiagonal and zeros elsewhere, $\mathbf{Q}$ is any unitary, column conjugate symmetric $M \times M$ matrix satisfying $\mathbf{J}\mathbf{Q}^* = \mathbf{Q}$ [2], $\mathbf{S} = \mathrm{E}\{\mathbf{s}(t)\mathbf{s}^H(t)\}$ is the $q \times q$

source waveform covariance matrix, $\mathbf{I}$ is the identity matrix, σ^2 is the noise variance, N is the number of snapshots, and $(\cdot)^*$ and $(\cdot)^H$ denote the transpose and the Hermitian transpose, respectively. The sparse matrices [1]-[3]

$$\mathbf{Q} = \frac{1}{\sqrt{2}} \begin{bmatrix} \mathbf{I} & j\mathbf{I} \\ \mathbf{J} & -j\mathbf{J} \end{bmatrix}, \quad \mathbf{Q} = \frac{1}{\sqrt{2}} \begin{bmatrix} \mathbf{I} & \mathbf{0} & j\mathbf{I} \\ \mathbf{0}^T & \sqrt{2} & \mathbf{0}^T \\ \mathbf{J} & \mathbf{0} & -j\mathbf{J} \end{bmatrix} \tag{8}$$

can be used for arrays with an even and odd number of sensors, respectively. Here, the zero vector $\mathbf{0} = (0, 0, \ldots, 0)^T$.

Define the eigendecompositions of the complex- and real-valued true covariance matrices in a standard way [2]

$$\mathbf{R} = \mathbf{V}\mathbf{\Pi}\mathbf{V}^H = \mathbf{V}_{\rm S}\mathbf{\Pi}_{\rm S}\mathbf{V}_{\rm S}^H + \sigma^2\,\mathbf{V}_{\rm N}\mathbf{V}_{\rm N}^H\,, \tag{9}$$

$$\mathbf{R}_{\rm FB} = \mathbf{U}\mathbf{\Lambda}\mathbf{U}^H = \mathbf{U}_{\rm S}\mathbf{\Lambda}_{\rm S}\mathbf{U}_{\rm S}^H + \sigma^2\,\mathbf{U}_{\rm N}\mathbf{U}_{\rm N}^H\,, \tag{10}$$

$$\mathbf{C} = \mathbf{E}\mathbf{\Gamma}\mathbf{E}^H = \mathbf{E}_{\rm S}\mathbf{\Gamma}_{\rm S}\mathbf{E}_{\rm S}^H + \sigma^2\,\mathbf{E}_{\rm N}\mathbf{E}_{\rm N}^H\,, \tag{11}$$

where $\mathbf{V}_{\rm S} = [\mathbf{v}_1, \ldots, \mathbf{v}_q]$, $\mathbf{V}_{\rm N} = [\mathbf{v}_{q+1}, \ldots, \mathbf{v}_M]$, $\mathbf{\Pi}_{\rm S} = {\rm diag}\{\pi_1, \ldots, \pi_q\}$, $\mathbf{U}_{\rm S} = [\mathbf{u}_1, \ldots, \mathbf{u}_q]$, $\mathbf{U}_{\rm N} = [\mathbf{u}_{q+1}, \ldots, \mathbf{u}_M]$, $\mathbf{\Lambda}_{\rm S} = {\rm diag}\{\lambda_1, \ldots, \lambda_q\}$, $\mathbf{E}_{\rm S} = [\mathbf{e}_1, \ldots, \mathbf{e}_q]$, $\mathbf{E}_{\rm N} = [\mathbf{e}_{q+1}, \ldots, \mathbf{e}_M]$, $\mathbf{\Gamma}_{\rm S} = {\rm diag}\{\gamma_1, \ldots, \gamma_q\}$, and the subscripts S and N stand for signal- and noise-subspace, respectively. The eigendecompositions of the sample covariance matrices can be defined as

$$\hat{\mathbf{R}} = \hat{\mathbf{V}}\hat{\mathbf{\Pi}}\hat{\mathbf{V}}^H = \hat{\mathbf{V}}_{\rm S}\hat{\mathbf{\Pi}}_{\rm S}\hat{\mathbf{V}}_{\rm S}^H + \hat{\mathbf{V}}_{\rm N}\hat{\mathbf{\Pi}}_{\rm N}\hat{\mathbf{V}}_{\rm N}^H\,, \tag{12}$$

$$\hat{\mathbf{R}}_{\rm FB} = \hat{\mathbf{U}}\hat{\mathbf{\Lambda}}\hat{\mathbf{U}}^H = \hat{\mathbf{U}}_{\rm S}\hat{\mathbf{\Lambda}}_{\rm S}\hat{\mathbf{U}}_{\rm S}^H + \hat{\mathbf{U}}_{\rm N}\hat{\mathbf{\Lambda}}_{\rm N}\hat{\mathbf{U}}_{\rm N}^H\,, \tag{13}$$

$$\hat{\mathbf{C}} = \hat{\mathbf{E}}\hat{\mathbf{\Gamma}}\hat{\mathbf{E}}^H = \hat{\mathbf{E}}_{\rm S}\hat{\mathbf{\Gamma}}_{\rm S}\hat{\mathbf{E}}_{\rm S}^H + \hat{\mathbf{E}}_{\rm N}\hat{\mathbf{\Gamma}}_{\rm N}\hat{\mathbf{E}}_{\rm N}^H \tag{14}$$

Writing the characteristic equation for the matrix $\hat{\mathbf{R}}_{\rm FB}$ as

$$\hat{\mathbf{R}}_{\rm FB}\hat{\mathbf{u}} = \hat{\lambda}\hat{\mathbf{u}}\,, \tag{15}$$

we obtain that

$$\mathbf{Q}^H\hat{\mathbf{R}}_{\rm FB}\hat{\mathbf{u}} = \mathbf{Q}^H\hat{\mathbf{R}}_{\rm FB}\mathbf{Q}\mathbf{Q}^H\hat{\mathbf{u}} = \hat{\mathbf{C}}\mathbf{Q}^H\hat{\mathbf{u}} = \hat{\lambda}\mathbf{Q}^H\hat{\mathbf{u}} \tag{16}$$

It is readily verifiable that equation (16) is the characteristic one for the real-valued covariance matrix $\hat{\mathbf{C}}$ in (4). Hence, the eigenvectors and eigenvalues of the matrices $\hat{\mathbf{C}}$ and $\hat{\mathbf{R}}_{\rm FB}$ are related as

$$\hat{\mathbf{E}} = \mathbf{Q}^H\hat{\mathbf{U}}\,, \quad \hat{\mathbf{\Gamma}} = \hat{\mathbf{\Lambda}} \tag{17}$$

The conventional root-MUSIC polynomial is given by

$$f_{\rm MUSIC}(z) = \mathbf{a}^T(1/z)\hat{\mathbf{V}}_{\rm N}\hat{\mathbf{V}}_{\rm N}^H\mathbf{a}(z)\,, \tag{18}$$

where $\mathbf{a}(z) = [1, z, \ldots, z^{M-1}]^T$, $z = e^{j\omega}$, and $\omega = \frac{2\pi}{\lambda}\,d\sin\theta$. Similarly to (18), the FB root-MUSIC polynomial can be used:

$$f_{\rm FB}(z) = \mathbf{a}^T(1/z)\hat{\mathbf{U}}_{\rm N}\hat{\mathbf{U}}_{\rm N}^H\mathbf{a}(z) \tag{19}$$

Using (17), we obtain that

$$\begin{aligned} f_{\rm FB}(z) &= \mathbf{a}^T(1/z)\mathbf{Q}\mathbf{Q}^H\hat{\mathbf{U}}_{\rm N}\hat{\mathbf{U}}_{\rm N}^H\mathbf{Q}\mathbf{Q}^H\mathbf{a}(z) \\ &= \mathbf{a}^T(1/z)\mathbf{Q}\hat{\mathbf{E}}_{\rm N}\hat{\mathbf{E}}_{\rm N}^T\mathbf{Q}^H\mathbf{a}(z) \\ &= \tilde{\mathbf{a}}^T(1/z)\hat{\mathbf{E}}_{\rm N}\hat{\mathbf{E}}_{\rm N}^T\tilde{\mathbf{a}}(z) = f_{\rm U}(z)\,, \end{aligned} \tag{20}$$

where the transformed manifold $\tilde{\mathbf{a}}(z) = \mathbf{Q}^H\mathbf{a}(z)$ should be exploited for the polynomial rooting in (20). The relationship between the standard and transformed manifolds follows from the expression for the real-valued true covariance matrix

$$\mathbf{C} = \mathbf{Q}^H\mathbf{A}\tilde{\mathbf{S}}\mathbf{A}^H\mathbf{Q} + \sigma^2\mathbf{Q}^H\mathbf{Q} = \tilde{\mathbf{A}}\tilde{\mathbf{S}}\tilde{\mathbf{A}}^H + \sigma^2\mathbf{I}\,, \tag{21}$$

where

$$\tilde{\mathbf{S}} = \frac{1}{2}\left(\mathbf{S} + \mathbf{D}\mathbf{S}^*\mathbf{D}^H\right)\,, \quad \tilde{\mathbf{A}} = \mathbf{Q}^H\mathbf{A}\,,$$

$$\mathbf{D} = {\rm diag}\{e^{-j\,\frac{2\pi}{\lambda}\,d(M-1)\sin\theta_1}, \ldots, e^{-j\,\frac{2\pi}{\lambda}\,d(M-1)\sin\theta_q}\}\,,$$

Let us term the polynomial (20) as the unitary root-MUSIC polynomial since it makes use of the eigendecomposition of the real-valued matrix $\hat{\mathbf{C}}$ rather than that of the complex-valued matrices $\hat{\mathbf{R}}$ and $\hat{\mathbf{R}}_{\rm FB}$. From (20), it is apparent that the FB and unitary root-MUSIC polynomials are identical. Therefore, the performance of unitary root-MUSIC does not depend on a particular choice of the unitary matrix $\mathbf{Q}$, although (8) seems to be an excellent choice because the matrix $\hat{\mathbf{C}}$ can be computed from the matrix $\hat{\mathbf{R}}_{\rm FB}$ with a very low computational demand. It is important to stress that, although both polynomials $f_{\rm FB}(z)$ and $f_{\rm U}(z)$ are proven to be identical, the calculation of the coefficients of $f_{\rm U}(z)$ is an easier operation (if implemented via the real-valued eigendecomposition (14)), because the real-valued eigendecomposition has a reduced computational cost relative to the complex one, approximately by a factor of four. Since the polynomial rooting is a much simpler operation than the eigendecomposition [5], we conclude that the overall computational complexity of unitary root-MUSIC is about four times lower than that of conventional root-MUSIC. We also stress that this conclusion cannot be extended to the unitary spectral MUSIC technique [1] because the main computational cost of spectral MUSIC is due to the demanding spectral search rather than the eigendecomposition.

3. ASYMPTOTIC PERFORMANCE

Let us introduce the eigenvector error

$$\mathbf{g}_i = \hat{\mathbf{e}}_i - \mathbf{e}_i\,, \quad i = 1, \ldots, q \tag{22}$$

Then, the following result holds [6]:

Lemma: The signal-subspace eigenvector estimation errors (22) are asymptotically (for a large number of snapshots N) jointly Gaussian distributed with zero means and covariance matrices given by

$$\begin{aligned} {\rm Cov}\,\{\mathbf{g}_i, \mathbf{g}_k\} = \frac{1}{N}\Bigg(&\sum_{\substack{l=1\\ l\neq i}}^{q}\sum_{\substack{p=1\\ p\neq k}}^{q}\frac{\Pi_{lpki}}{(\gamma_i-\gamma_l)(\gamma_k-\gamma_p)}\,\mathbf{e}_l\mathbf{e}_p^T \\ &+ \frac{\gamma_i\,\sigma^2}{2\,(\gamma_i-\sigma^2)^2}\,\mathbf{E}_{\rm N}\mathbf{E}_{\rm N}^T\,\delta_{ik}\Bigg)\,, \end{aligned} \tag{23}$$

where $\Pi_{lpki} = \frac{1}{2}(\gamma_i\gamma_p\delta_{ik}\delta_{lp} + \gamma_i\gamma_k\delta_{ip}\delta_{kl} + \mathbf{w}_l^T(\mathbf{e}_p\mathbf{e}_k^T + \mathbf{e}_k\mathbf{e}_p^T)\mathbf{w}_i)$, $\mathbf{w}_i = {\rm Im}\left\{\mathbf{Q}^H\mathbf{R}\mathbf{Q}\right\}\mathbf{e}_i$, $1 \le i,k \le q$, and δ_{ik} denotes the Kronecker delta.

Following [4], we obtain that the DOA estimation Mean Square Error (MSE) of unitary root-MUSIC is given by

$${\rm E}\left\{(\hat{\theta}_i - \theta_i)^2\right\} = \left(\frac{\lambda}{4\pi d\cos\theta_i}\right)^2\frac{{\rm E}\left\{\hat{G}(\omega_i)\right\}}{\left(\tilde{\mathbf{d}}^H(\omega_i)\mathbf{E}_{\rm N}\mathbf{E}_{\rm N}^T\tilde{\mathbf{d}}(\omega_i)\right)^2}\,, \tag{24}$$

where $\tilde{\mathbf{d}}(\omega) = d\tilde{\mathbf{a}}(\omega)/d\omega$,

$$\hat{G} = 2\mathrm{Re}\left\{\left(\tilde{\mathbf{d}}^H\left(\sum_{k=1}^{q}(\mathbf{e}_k\mathbf{g}_k^T+\mathbf{g}_k\mathbf{e}_k^T)\right)\tilde{\mathbf{a}}\right)^2\right\} + 2\left|\tilde{\mathbf{d}}^H\left(\sum_{k=1}^{q}(\mathbf{e}_k\mathbf{g}_k^T+\mathbf{g}_k\mathbf{e}_k^T)\right)\tilde{\mathbf{a}}\right|^2, \quad (25)$$

and, for the sake of brevity, we denote $\hat{G} = \hat{G}(\omega_i)$, $\tilde{\mathbf{a}} = \tilde{\mathbf{a}}(\omega_i)$, and $\tilde{\mathbf{d}} = \tilde{\mathbf{d}}(\omega_i)$. Using (23)-(24) and the readily verifiable equations $\mathbf{E}_{\mathrm{N}}^T\tilde{\mathbf{a}} = \mathbf{0}$ and

$$\Pi_{iplk} = \Pi_{kpli} = \Pi_{ilpk} = \Pi_{klpi}\,, \quad (26)$$

we obtain that

$$\mathrm{E}\left\{\hat{G}\right\} = \frac{\sigma^2}{N}\sum_{k=1}^{q}\frac{\gamma_k}{(\gamma_k-\sigma^2)^2}\left(\mathrm{Re}\left\{(\mathbf{e}_k^T\tilde{\mathbf{a}})^2\,\tilde{\mathbf{d}}^H\mathbf{E}_{\mathrm{N}}\mathbf{E}_{\mathrm{N}}^T\tilde{\mathbf{d}}^*\right\} + |\mathbf{e}_k^T\tilde{\mathbf{a}}|^2\,\tilde{\mathbf{d}}^H\mathbf{E}_{\mathrm{N}}\mathbf{E}_{\mathrm{N}}^T\tilde{\mathbf{d}}\right) \quad (27)$$

In can be shown that $\tilde{\mathbf{d}}(\omega) = j\,\mathbf{Q}^H\mathbf{\Delta}\,\mathbf{Q}\,\tilde{\mathbf{a}}(\omega)$ where $\mathbf{\Delta} = \mathrm{diag}\{0,1,2,\ldots,M-1\}$. Also, it can be readily verified that $\mathbf{J}\mathbf{a}(\omega) = z^{M-1}\mathbf{a}^*(\omega)$, $\mathbf{J}\mathbf{Q}^* = \mathbf{Q}$, and $\mathbf{U}_{\mathrm{N}}^T = \mathbf{U}_{\mathrm{N}}^H\mathbf{J}$. Using all these properties and (17), we can prove that

$$(\mathbf{e}_k^T\tilde{\mathbf{a}})^2\,\tilde{\mathbf{d}}^H\mathbf{E}_{\mathrm{N}}\mathbf{E}_{\mathrm{N}}^T\tilde{\mathbf{d}}^* = -j|\mathbf{e}_k^T\tilde{\mathbf{a}}|^2(\tilde{\mathbf{d}}^H\mathbf{E}_{\mathrm{N}}\mathbf{E}_{\mathrm{N}}^T\mathbf{Q}^H\mathbf{J}\mathbf{\Delta}\mathbf{J}\mathbf{Q}\tilde{\mathbf{a}}) \quad (28)$$

Using the identities $\mathbf{E}_{\mathrm{N}}^T\tilde{\mathbf{a}} = \mathbf{0}$ and $\mathbf{\Delta} - (M-1)\mathbf{I} = -\mathbf{J}\mathbf{\Delta}\mathbf{J}$, it is easy to show that

$$-j\,\mathbf{E}_{\mathrm{N}}^T\mathbf{Q}^H\mathbf{J}\mathbf{\Delta}\mathbf{J}\mathbf{Q}\tilde{\mathbf{a}} = \mathbf{E}_{\mathrm{N}}^T\tilde{\mathbf{d}} \quad (29)$$

Inserting (29) into (28), we obtain

$$(\mathbf{e}_k^T\tilde{\mathbf{a}})^2\,\tilde{\mathbf{d}}^H\mathbf{E}_{\mathrm{N}}\mathbf{E}_{\mathrm{N}}^T\tilde{\mathbf{d}}^* = |\mathbf{e}_k^T\tilde{\mathbf{a}}|^2\,\tilde{\mathbf{d}}^H\mathbf{E}_{\mathrm{N}}\mathbf{E}_{\mathrm{N}}^T\tilde{\mathbf{d}} \quad (30)$$

Substituting 30) into (27) and using (17), we derive from (24) the final expression for the DOA estimation MSE:

$$\mathrm{E}\left\{(\hat{\theta}_i-\theta_i)^2\right\} = \left(\frac{\lambda}{4\pi d\cos\theta_i}\right)^2\frac{\sigma^2\sum_{k=1}^{q}\frac{\lambda_k}{(\lambda_k-\sigma^2)^2}|\mathbf{u}_k^H\mathbf{a}|^2}{N\,\mathbf{d}^H\mathbf{U}_{\mathrm{N}}\mathbf{U}_{\mathrm{N}}^H\mathbf{d}}\,, \quad (31)$$

where $\mathbf{d}(\omega) = d\mathbf{a}(\omega)/d\omega$ and the simplified notations $\mathbf{a} = \mathbf{a}(\omega_i)$ and $\mathbf{d} = \mathbf{d}(\omega_i)$ are used. Comparing (31) with equations (26) and (28) in [4], we see that the only difference between the MSE's of the conventional and unitary root-MUSIC algorithms is that our expression (31) for the unitary root-MUSIC MSE contains the eigenvectors and eigenvalues of the FB covariance matrix $\mathbf{R}_{\mathrm{FB}}$, whereas the aforementioned expressions in [4] contain the eigenvectors and eigenvalues of the conventional covariance matrix $\mathbf{R}$. Apparently, in uncorrelated source scenarios $\mathbf{R} = \mathbf{R}_{\mathrm{FB}}$, and, therefore, we conclude that the asymptotic performances of the unitary and conventional root-MUSIC algorithms are identical in this case. However, in multipath scenarios, where the sources may be correlated or coherent, the asymptotic performance of unitary root-MUSIC is better than that of conventional root-MUSIC due to the FB averaging effect. This fact is clearly demonstrated in the next section by means of comparison of our analytical and simulation results.

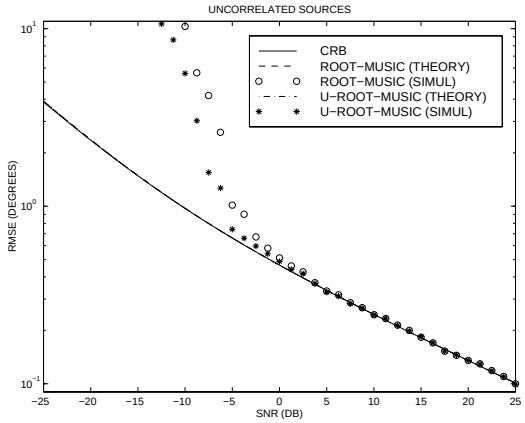

Figure 1: RMSE's vs. the SNR in the first example.

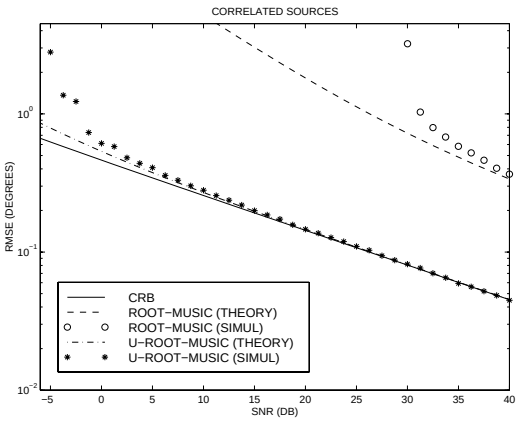

Figure 2: RMSE's vs. the SNR in the second example.

4. SIMULATIONS

We consider a ULA of $M = 10$ omnidirectional sensors with the half-wavelength interelement spacing, and two equally powered narrowband sources with $\theta_1 = 10°$ and $\theta_2 = 15°$. A total of 1000 independent simulation runs have been used and the number of snapshots taken is $N = 100$. In both our examples, the experimental DOA estimation Root-Mean-Square Errors (RMSE's) have been compared with the stochastic Cramér-Rao Bound (CRB) and with the results of our asymptotic analysis.

In the first and second examples, we modeled two uncorrelated and correlated sources (with the correlation coefficient equal to 0.99 and zero intersource phase in the first array sensor), respectively. Figures 1 and 2 show the results for these examples.

From these figures, we remark that there is an excellent correspondence of the theoretical curves and experimental points at high SNR values. As expected, for uncorrelated sources the asymptotic performances of both algorithms are similar. However, from the example with the correlated sources, we observe that the unitary root-MUSIC algorithm performs asymptotically much better. Moreover, in both examples unitary root-MUSIC has essentially lower SNR threshold than conventional root-MUSIC.

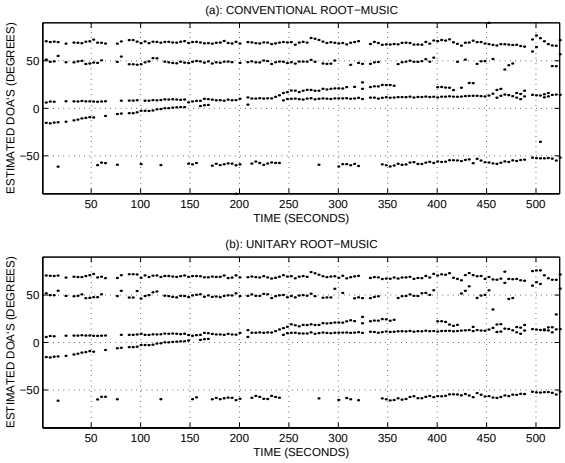

Figure 3: Real sonar data processing.

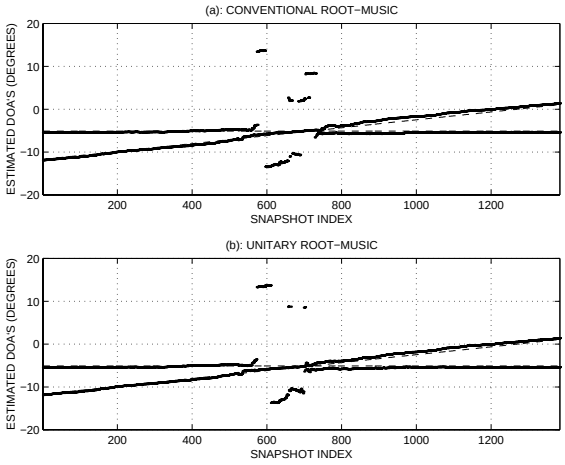

Figure 4: Real ultrasonic data processing.

5. EXPERIMENTAL STUDY

In our experimental part of study, real sonar and ultrasonic ULA data have been used. The sonar experiments were conducted by STN Atlas Elektronik, Bremen, in October 1983, in the Bornholm Deep, Baltic Sea. A horizontal ULA of 15 hydrophones was towed by a surface ship. The sea depth at the experimental site was about $60 - 65$ m. The towed receiving array had the interelement spacing $d = 2.56$ m and the sampling frequency $f_s = 1024$ Hz after lowpass filtering with the cutoff 256 Hz. The narrowband snapshots with the 4 Hz bandwidth have been formed from these wideband data after the DFT using the frequency bin $f = 240$ Hz. The sequence of covariance matrices has been estimated using nonoverlapping sliding windows with four seconds duration.

Figs. 3 (a) and (b) show the results of real sonar data processing using the conventional and unitary root-MUSIC methods, respectively. From these plots, we see that both algorithms have nearly identical performance.

The ultrasonic data were recorded at University of Wyoming Source Tracking Array Testbed (UW STAT) [7]. These narrowband 6-element array data are available on the World Wide Web at `http://wwweng.uwyo.edu/electrical/array.html`. They have the carrier frequency 40 kHz and the signal bandwidth 200 Hz. The receiving ULA with the interelement spacing 2.1λ has been used.

A rectangular (maximal-overlap) sliding window with $N = 150$ snapshots has been used to estimate the source trajectories. The results for conventional and unitary root-MUSIC are shown in Fig. 4 (a) and (b), respectively. From these plots, we observe that both algorithms have serious problems when the sources become closely spaced. However, from Fig. 4 we see that unitary root-MUSIC has better threshold performance than conventional root-MUSIC.

6. CONCLUSIONS

The real-valued (unitary) root-MUSIC algorithm has been developed for direction finding in sensor arrays. The unitary and FB root-MUSIC polynomials have been shown to be identical, but unitary root-MUSIC provides essentially lower computational complexity than the conventional root-MUSIC technique. Closed-form expressions for the large sample MSE of unitary root-MUSIC have been derived and compared with the well-known asymptotic results for conventional root-MUSIC. It has been shown that unitary root-MUSIC performs asymptotically identically to or better than conventional root-MUSIC, depending on source mutual correlation. Additionally, the results of our simulations and real data processing have shown the better performance of unitary root-MUSIC in the threshold domain. Since the unitary and conventional root-MUSIC techniques are both applicable in the ULA case, we conclude that unitary root-MUSIC should be always preferred by the user to conventional root-MUSIC.

7. REFERENCES

[1] K.C. Huarng and C.C. Yeh, "A unitary transformation method for angle of arrival estimation," *IEEE Trans. ASSP*, **39**, pp. 975-977, 1991.

[2] D.A. Linebarger, R.D. DeGroat, and E.M. Dowling, "Efficient direction-finding methods employing forward-backward averaging," *IEEE Trans. SP*, **42**, pp. 2136-2145, 1994.

[3] M. Haardt and J.A. Nossek, "Unitary ESPRIT: How to obtain increased estimation accuracy with a reduced computational burden," *IEEE Trans. SP*, **43**, pp. 1232-1242, 1995.

[4] B.D. Rao and K.V.S. Hari, "Performance analysis of root-MUSIC," *IEEE Trans. ASSP*, **37**, pp. 1939-1949, 1989.

[5] M. Lang and B-C. Frenzel, "Polynomial root finding," *IEEE Signal Processing Letters*, **1**, pp. 141-143, 1994.

[6] G.M. Kautz and M. Zoltowski, "Performance analysis of MUSIC employing conjugate symmetric beamformers," *IEEE Trans. SP*, **43**, pp. 737-748, 1995.

[7] J.W. Pierre, E.D. Scott, and M.P. Hays, "A sensor array testbed for source tracking algorithms," *Proc. ICASSP'97*, Munich, pp. 3769-3772, 1997.